Generative adversarial network-enabled learning scheme for power grid vulnerability analysis

Ying Liu, Tao Ye, Zhixiang Zeng,
Yingbin Zhang, Guoshi Wang and Ning Chen

Hainan Power Grid Co., Ltd.,
China Southern Power Grid,
Hainan, China
Email: 313619456@qq.com
Email: yet@hn.csg.cn
Email: zengzx2@hn.csg.cn
Email: zhangyb2@hn.csg.cn
Email: 245545383@qq.com
Email: chenn@hn.csg.cn

Cunli Mao

Faculty of Information Engineering and Automation,
Kunming University and Science Technology,
Kunming, 650500, China
Email: maocunli@163.com

Xiaohui Yuan*

Department of Computer Science and Engineering,
University of North Texas,
Denton, Texas, 76207, USA
Email: xiaohui.yuan@unt.edu
*Corresponding author

Abstract: Real measurements of power grids are usually limited for research and modelling of extreme events such as the impact of typhoons due to confidentiality concerns. To overcome the dearth of valuable, trustworthy data, this paper proposes an adaptive learning method based on the generative adversarial network. To obtain informative examples, the falsely classified examples together with examples that are correctly classified with low confidence are used to train a GAN for producing synthetic examples to reinforce the learning. The new power grid examples are selected according to the likelihood of the true data distribution. An evaluation was conducted with data acquired by the China Southern Power Grid in Hainan. Most significantly, the performance of detecting the occurrence of a power grid fault under the impact of typhoons is greatly improved. It was demonstrated that the proposed method improved the performance of predicting power grid fault in extreme events by 8.9%. Using the modulated GAN network, the synthetic data closely follows the distribution of the real data as indicated by large p-values. Our method takes minutes to complete training a model, which enables an efficient response to disasters with modern computing facilities such as edge computing.

Keywords: power grid; generative adversarial network; GAN; classification; rare events.

Reference to this paper should be made as follows: Liu, Y., Ye, T., Zeng, Z., Zhang, Y., Wang, G., Chen, N., Mao, C. and Yuan, X. (2021) 'Generative adversarial network-enabled learning scheme for power grid vulnerability analysis', *Int. J. Web and Grid Services*, Vol. 17, No. 2, pp.138–151.

Biographical notes: Ying Liu received his Master's degree in Computer Application Technology from Chongqing University of Technology. He works in the Digital Department of Hainan Power Grid Co., Ltd., and his research interests include informatisation planning, computer vision and data mining.

Tao Ye graduated with a Bachelor's degree from Huazhong University of Science and Technology. He works in the Safety Supervision Department of Hainan Power Grid Co., Ltd. His research interests include computer vision, data mining, emergency management, and safety risk management system.

Zhixiang Zeng graduated with a Bachelor's degree from China University of Mining and Technology. He works in the Information and Communication Branch of Hainan Power Grid Co., Ltd. His research interests include information security, computer vision and data mining.

Yingbin Zhang graduated from Communication University of China. He works in the Information and Communication Branch of Hainan Power Grid Co., Ltd. His research interests include information and communication technology, computer vision and data mining.

Guoshi Wang received his Master's degree in Computer Science and Technology from Beijing University of Posts and Telecommunications. He works in the Information and Communication Branch of Hainan Power Grid Co., Ltd. and his research interests include big data, cloud computing and computer vision.

Ning Chen received her Master's degree from Beijing University of Aeronautics and Astronautics. She is working in the Information and Communication Branch of Hainan Power Grid Co., Ltd., and her research interests include computer vision and data mining.

Cunli Mao received his PhD degree from Kunming University of Science and Technology in 2014. He is currently an associate professor with the School of Information Engineering and Automation, Kunming University of Science and Technology, China. He has been a CCF member since 2011. His research interests include nature language processing, image processing, machine learning and information retrieval.

Xiaohui Yuan received his BS degree in Electrical Engineering from Hefei University of Technology, China, in 1996 and his PhD in Computer Science from Tulane University in 2004. He is currently an Associate Professor at the University of North Texas. His research interests include computer vision, artificial intelligence, data mining, and machine learning. His research findings have been published in more than 160 peer-reviewed papers. He is the Editor-in-Chief of the *International Journal of Smart Sensor Technologies and Applications*, serves on the editorial board of several international journals, and chairs several international conferences. He was a recipient of the Ralph E. Powe Junior Faculty Enhancement Award in 2008.

1 Introduction

After natural disasters such as typhoons and flooding hit the coastal cities, restoring power is a vital component to disaster response for running hospitals, providing light and warmth to citizens, establishing communications, etc. (Elhoseny et al., 2018). There is apparently a growing need for credible data to support the risk and sustainability analysis of the impact of natural disasters on the complex electricity network (Fan et al., 2016; Elhoseny et al., 2014). The rapid development of internet of things introduces new values to the existing sensor network in the power grid by injecting smart devices and intelligent applications, which improves the quality of data. On the other hand, the real measurement of power grids is usually confidential and subject to protection according to regional or national regulations or laws such as the Critical Energy/Electric Infrastructure Information Regulations (Federal Energy Regulatory Commission, https://www.ferc.gov/legal/maj-ord-reg/land-docs/ceii-rule.asp). To overcome the dearth of valuable data, the demand is usually responded by simulation software. However, physical models often face challenges of model complexity and deviation from the real measurements. Alternatively, model-free methods created from the available, but limited real data are promising for generating synthetic data by modelling the behaviour of the real power grid system (Yuan et al., 2018). An assumption is usually made that the space between two examples of a class is filled with examples of the same class. Hence, sophisticated data interpolation methods have been developed and used to augment the real examples in ensemble learning methods for circumventing the data imbalance problem (Yuan and Abouelenien, 2015). Such an assumption is plausible, but a large portion of the newly generated synthetic examples are distance to the decision boundary, which provides limited new information to shape the learner.

To generate credible datasets that better capture the underlying systems, learning-based methods have been developed, among which generative adversarial network (GAN) demonstrated much superior performance in producing synthetic data following a competitive, self-verification strategy (Goodfellow et al., 2014). Two competing components are employed in a GAN model: a generator and a discriminator, where the training of the generator is to maximise the probability of the discriminator. The goal is to minimise the difference-based costs between real image examples and the synthesised ones. Following this idea, Mathieu et al. (2016) train a convolutional network to generate video frames that preserve the image sharpness by combining adversarial training and gradient-based loss function. The network was used to generate future frames provided with an input video sequence. Yi et al. (2017) develop a dual-GAN to translate images by training a primal GAN and a dual GAN with two sets of unlabeled images of different domains. The primal GAN learns to translate images from one domain to those in a second domain, while the dual GAN learns to reverse the translation. To circumvent the vanishing gradients that cause training instability, improved methods have been developed such as least square GAN (Mao et al., 2017) and Wasserstein GAN (Arjovsky et al., 2017; Gulrajani et al., 2017).

The success of GAN in producing imagery and videos excited researchers to extend the idea to other data modalities and applications. Reed et al. (2016) extended the GAN model for image synthesis that translates text descriptions to plausible images of birds and flowers. In the proposed method, a manifold interpolation regulariser for the GAN generator was developed, which generates text embeddings by interpolating between embeddings of the captions of the training set. Yang et al. (2017) applied GAN for

symbolic domain music generation with multiple channels. The proposed MidiNet employs convolutions on a 2D matrix representing the presence of notes over different time steps to generate melodies in a successive manner. A discriminator is used to model the distribution of melodies. Chen et al. (2018) employed GAN to learn renewable energy production patterns for a large number of correlated resources. The proposed method successfully synthesised photovoltaic power and wind profiles in both temporal and spatial dimensions and new examples retained the diversity.

This paper aims to address the problem of dearth of valuable examples to model real-world systems under the influence of rare events, specifically in the case of power-grid under natural disasters of typhoons. In addition, the fidelity of the training examples is of paramount importance in the development of a reliable model. In response to these problems, we present a learning method that leverages synthetic examples to improve the characterisation of systems under extreme events. To obtain informative examples for training a model, the falsely classified examples by a base learner together with examples that are correctly classified with low confidence are used to train a GAN network for producing synthetic examples to reinforce the learning process. A filtering strategy based on the significance of the training examples is devised. The new power grid examples are selected according to the likelihood of the true data distribution. Our proposed adaptive learning strategy supports the analysis of typhoon impact based on different conditions of interest with scarce examples.

The rest of this article is organised as follows: Section 2 gives an overview of our proposed method and presents the details of the key components. Section 3 discusses the experimental results using a real dataset acquired from the power grid of Hainan, China during a severe typhoon disaster. We examine our proposed method in the aspects of model performance, data fidelity and computational efficiency. In the evaluation of model performance, we compared the base learner performance to the proposed method with various parameter settings and performance metrics. Section 4 concludes this paper with a summary of the proposed method and our key findings.

2 Adaptive learning with GAN

Because of the limited training examples, especially the ones that represent rare, but important, events, our proposed method employs GAN to produce additional examples for model training. The question is what examples to be synthesised. The basic idea of the GAN is that the synthetic data are representative of the real examples if the distribution of the synthetic data is highly similar to that of the real examples. Hence, a well-trained GAN generates more examples to supplement the learning of the minority class, i.e., the class with much less number of examples, as well as the majority class, which in part circumvents the data imbalance problem. However, employing the expanded training dataset for model training still faces the problem of lacking representative examples that are key to differentiate the classes. The idea of our proposed method is to build a GAN from the most confusing examples, which is used to enrich the training set with informative cases.

Figure 1 illustrates the overall architecture of our proposed method. Our method takes training examples and random noise as input to fuel the modelling of both a classifier (i.e., a learner) and the GAN network. After the learner is trained, it is applied to all the examples to make a prediction. Using the confidence of the prediction, examples are

selected and used as input for the training of the GAN network. By minimising the difference between the new instances produced by the generator, a GAN network is created to mimic the power grid where the real data are acquired. The random input for the GAN network is gradually updated to model the distribution that favours the production of minority examples. To update the learning, the most representative examples are used, together with the real examples, to circumvent the lack of examples and innate data imbalance. In the rest of this section, we present the details of our example filtering strategy and modulated the GAN network.

Figure 1 The architecture of our proposed adaptive learning method (see online version for colours)

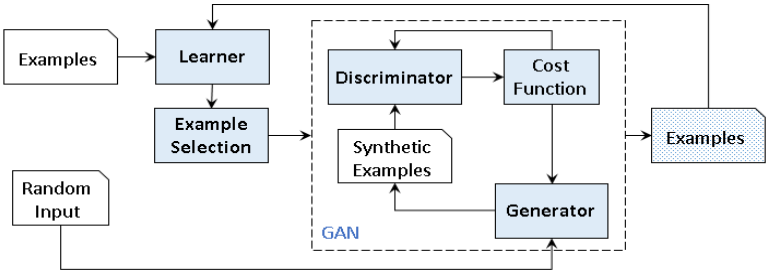

2.1 Example filtering strategy

Provided with a set of examples $X = \{x_1, x_2, \ldots, x_N\}$, a learner f is trained that maps x_i into a lower dimensional vector y_i:

$$y_i \leftarrow f(x_i).$$

For the binary classification problems, $y_i \in \{-1, 1\}$. The confidence of a prediction of an instance x_j, denoted with $c(x_j)$, is proportional to the distance of x_j to the decision boundary, i.e., $c(x_j) \propto \|f(x_j)\|$ where c denotes the confidence and $\|\cdot\|$ denotes the distance function. To regulate the range of confidence, the confidence follows the sigmoid function as follows:

$$c(x_j) = \frac{2e^{\|f(x_j)\|}}{1+e^{\|f(x_j)\|}}. \tag{1}$$

It is expected that the real examples selected for training a GAN network help to alleviate the uncertainty and the lack of representation of the minority class. Hence, given the ratio of the class sizes γ, $\gamma \leq 1$, the significance of an example x_j is computed as the inverse of the product of the confidence and imbalance ratio:

$$s(x_j) = \frac{1}{\gamma(y_j)(1+c(x_j))} \tag{2}$$

where $\gamma(y_j)$ denotes the imbalance ratio as a function of class y_j of example x_j, and we have

$$\gamma(y_j) = \begin{cases} \gamma, & \text{if } x_j \text{ is a minority class example} \\ \gamma^{-1}, & \text{if } x_j \text{ is a majority class example} \end{cases}.$$

The range of confidence $c(x_j)$ is in [0 1]. To avoid the singular case when $c(x_j)$ equals zero, the confidence is rescaled by adding a one. The probability of example filtering, denoted with $p(x_j)$ is proportional to its significance $s(x_j)$

$$p(x_j) = s(x_j) / S \tag{3}$$

where S is a normalisation factor

$$S = \sum_j s(x_j).$$

The training examples for the GAN network are hence randomly drawn from the population of the real dataset following the above probability.

2.2 Modulated GAN network

The GAN module consists of two major components: a generative network (a.k.a. generator) and a discriminative network (a.k.a. discriminator). Given a random input z, the generator g synthesises an instance $\dot{x} = g(z)$. The discriminator d is trained to differentiate if an input instance is a synthetic example or a real one, and returns a probability of this instance to be a real sample. The error of the discriminator is expressed as the sum of error of the real and synthetic examples:

$$\begin{aligned} E(g, d) &= E_x \log d(x) + E_z \log\left(1 - d\left(g(z)\right)\right) \\ &= E_x \log d(x) + E_x \log\left(1 - d(x)\right) \end{aligned} \tag{4}$$

The network is trained such that the discriminator maximises the probability of assigning the correct label to both the real examples and the newly generated instances by the generator. Simultaneously, the generator is trained to minimise $\log(1 - d(g(z)))$, that is,

$$\min_g \max_d E(g, d). \tag{5}$$

In practice, this objective function may provide an insufficient gradient to learn a plausible generator. In the early stage of the training process when the generator is fairly poor, the discriminator can reject synthetic examples with high confidence, which saturates $\log(1 - d(g(z)))$. Hence, instead of minimising $\log(1 - d(g(z)))$, the learning process maximises $\log d(g(z))$. This objective function provides stronger gradients early in learning.

In addition to feeding the GAN module with the significant examples selected via the filtering process, we introduce a modulated random input to favour the generation of examples of the minority class. Let q denote the probability distribution of the random input z, which follows Gaussian distribution

$$q(z; \mu, \sigma) = \mathcal{N}(\mu, \sigma). \tag{6}$$

As the generator synthesises new instances, the random inputs z_k that result in minority examples are used to constrain the probability by updating μ and σ of q. Hence, the objective function becomes

$$\min_{g} \max_{d} E(g, d) \text{ s.t. } q(z) \sim \mathcal{N}(\dot{\mu}, \dot{\sigma}) \tag{7}$$

where the Gaussian parameters $\dot{\mu}$ and $\dot{\sigma}$ are computed based on the random inputs resulted in minority class examples.

3 Results and discussion

3.1 Experimental data and settings

The data used in our study were collected over a period of 48 hours on July 17, 2014, at the transformer stations in Hainan, when Typhoon Rammasun made landfall near Wenchang in Mainland China. Figure 2 illustrates the area of study with a visualisation of the tracks of typhoons in the western Pacific Ocean in 2014 and the topology of the power grid of Hainan. Typhoon Rammasun was a category 5 super typhoon and among the strongest skirted Hainan, China. It produced strong gales that were over 100 miles per hour and heavy rain, which caused severe damage to the infrastructure of several countries along its path including the Philippines, China, Vietnam, and the Mariana Islands. This presents a typical scenario for the study of typhoon impact to the power grid.

In our dataset, each record consists of 13 properties including sensor outputs such as coil voltage ratio, current ratio, temperature, core vibration magnitude, etc., as well as weather readings such as average wind speed, precipitation, etc. The range of each property is normalised to the same scale to suppress the difference in value magnitude. The dataset consists of 612 records that report power faults and 6,030 records that document the normal performance. In our implementation, without loss of generality, we used a support vector machine (SVM) as the learner in our architecture to model power grid faults under typhoon. The SVM used polynomial kernel in our experiments.

Our results are reported with the evaluation metrics that differentiate the rare events (i.e., the minority class) from the regular normal operation, which include sensitivity ε, specificity ϱ, and balanced accuracy $\mathcal{A}$. The formulas of these metrics are given as follows:

$$\text{Sensitivity: } \varepsilon = \frac{TP}{TP + FN}$$

$$\text{Specificity: } \varrho = \frac{TN}{TN + FP}$$

$$\text{Balanced accuracy: } \mathcal{A} = \frac{1}{2}\left(\frac{TP}{P} + \frac{TN}{N}\right)$$

where P and N denote the number of positive and negative examples, respectively, TP and TN denote the true positive and true negative predictions, respectively, FP and FN denote the false positive and false negative predictions, respectively. Compared to widely

used accuracy, balanced accuracy is a performance metric for a model, whether or not the data is imbalanced, and hence, provides greater interpretative power.

Figure 2 Area of study (see online version for colours)

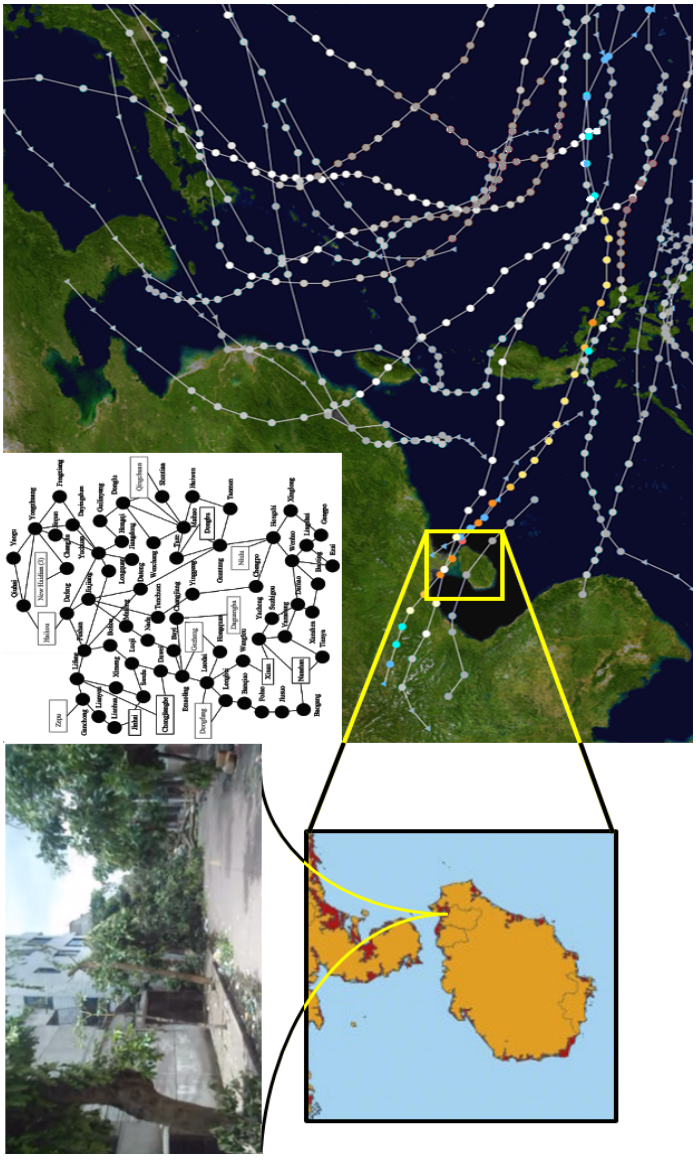

Notes: The bottom-right depicts the tracks of typhoons in the western Pacific Ocean in 2014. The track of Typhoon Rammasun in 2014 is highlighted in colour; whereas the other tracks of typhoons are shown in greyscale. The yellow box highlights the area of study: Hainan Province, China. The lower-left shows the degree of impact by Typhoon Rammasun in 2014. A local view is shown on the top-left corner of figure. The topology of the power grid of Hainan is shown in the top-middle portion of figure.

3.2 Performance analysis

Out of all the examples in our dataset, 600 minority examples that represent faulty cases and 6,000 majority examples that represent normal operations were randomly selected and used in the rest of our experiments. The imbalance ratio γ is hence 0.1. To understand the effectiveness of our proposed method, we conducted experiments using the baseline method SVM and our proposed method that generated different amounts of synthetic examples. In the evaluation of our proposed method, we conducted experiments using three contrasting scenarios:

1 using the modulated GAN to generate synthetic examples and keeping the imbalance ratio, i.e., $\gamma = 0.1$

2 using the modulated GAN to generate more synthetic minority examples to reduce the imbalance ratio to 0.5, i.e., $\gamma = 0.5$

3 using the modulated GAN to generate more synthetic minority examples to achieve a balance between classes, i.e., $\gamma = 1$.

Given the limited number of minority class examples, four-fold cross-validation was conducted for each method/scenario to ensure a sufficient number of examples were available for evaluation.

Table 1 The performance of the baseline and our proposed methods

	Accuracy	*Sensitivity*	*Specificity*	*Balanced accuracy*
Baseline SVM $\gamma = 0.1$	0.987	0.933	0.993	0.963
	0.984	0.907	0.992	0.949
	0.984	0.900	0.993	0.946
	0.982	0.873	0.993	0.933
	0.985	*0.903*	*0.993*	*0.948*
Our method $\gamma = 0.1$	0.988	0.950	0.996	0.973
	0.985	0.960	0.990	0.975
	0.984	0.945	0.992	0.969
	0.983	0.930	0.993	0.962
	0.985	*0.946*	*0.993*	*0.970*
Our method $\gamma = 0.5$	0.983	0.982	0.983	0.983
	0.984	0.978	0.987	0.983
	0.985	0.982	0.986	0.984
	0.987	0.98	0.991	0.986
	0.985	*0.981*	*0.987*	*0.984*
Our method $\gamma = 1$	0.985	0.983	0.987	0.985
	0.988	0.983	0.993	0.988
	0.985	0.990	0.980	0.985
	0.980	0.977	0.983	0.980
	0.985	*0.983*	*0.986*	*0.985*

Table 1 reports our experimental results in terms of accuracy, sensitivity, specificity and balanced accuracy. The average performance is highlighted in italic font. By comparing the average sensitivity of the baseline method and that of our method with $\gamma = 1$, we see a significant improvement from 0.903 to 0.983, which is at a rate of 8.9%. That is our proposed method demonstrated much-improved performance over predicting possible power grid faults. As the dataset became balanced, the specificity reduced slightly. With $\gamma = 0.1$, the average specificity of the baseline method and our proposed method was 0.993, which reduced to 0.987 for $\gamma = 0.5$ and 0.986 for $\gamma = 1$. The reduction rate is at most 0.7%, which is much less significant compared to the improvement of the sensitivity.

Indeed, when taking into account the changes in both sensitivity and specificity, we see a constant improvement in terms of balanced accuracy as γ increases. The average balanced accuracy of the baseline method is 0.948; whereas the average balanced accuracy of our proposed method when $\gamma = 0.1$, 0.5, and 1 is 0.97, 0.984 and 0.985, respectively. The maximum improvement rate over the average balanced accuracy is 3.9%. It is worth mentioning that by keeping the same imbalance ratio of the newly created synthetic examples, our method improved the average balanced accuracy by 2.3% from the baseline. It is evident that the positive change comes from the enrichment of the training examples.

Throughout all the scenarios, the average accuracy remains at 0.985. Clearly, it is not a good indicator to evaluate the performance of imbalanced datasets. In contrast, balanced accuracy better illustrates the performance variations among imbalance ratios. As γ increases, the balanced average approaches accuracy. When γ becomes one, balanced accuracy reduces to the conventional accuracy metric and reports the same value.

3.3 Data fidelity

An interesting question is how close the synthetic examples mimic the real data. For low dimensional datasets, a visualisation could reveal how similar are the distributions formed by the synthetic data and by the real data. However, our dataset consists of instances with 13 dimensions, which makes it impossible to directly visualise the data distribution. Hence, we conducted our evaluation using the one-way ANOVA analysis.

Figure 3 illustrates the distribution of p-values of the datasets. Figure 3(a) shows the p-value distribution of the minority class for the real and synthetic datasets. Each bar gives the p-value assuming that the null hypothesis is correct. The null hypothesis is that the two datasets are drawn from the same distribution. If the p-value is less than a significance level (typically 0.05 or 0.01), it suggests that the null hypothesis may be rejected, i.e., the two datasets are of different distributions. As shown in this plot, the p-values are fairly large (greater than 0.1). In fact, the average p-value is 0.254, which is much greater than a typical significant level and provides strong support that the two datasets are probably following a similar, if not the same, distribution. Figure 3(b) shows the p-value distribution of the majority class for the real and synthetic datasets. We clearly see a similar pattern among the p-values of all 13 properties. The average p-value for the majority class is 0.205 between the real and synthetic data. It is evident that the modulated GAN network produced credible data for developing a model.

Figure 3 One-way ANOVA analysis of the datasets, (a) minority (real vs. synthetic) (b) majority (real vs. synthetic) (c) real data (minority vs. majority) (d) synthetic data (minority vs. majority) (see online version for colours)

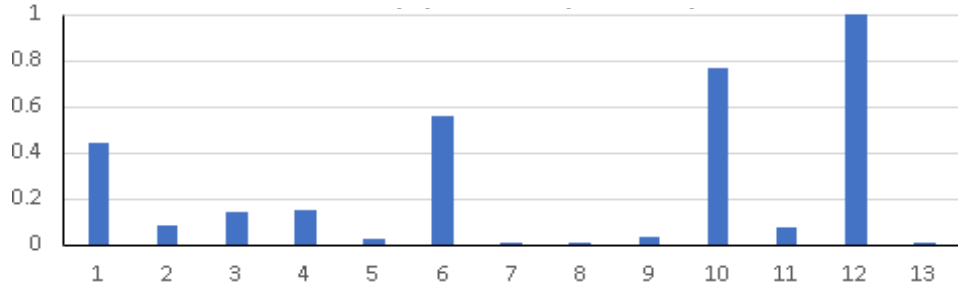

(a)

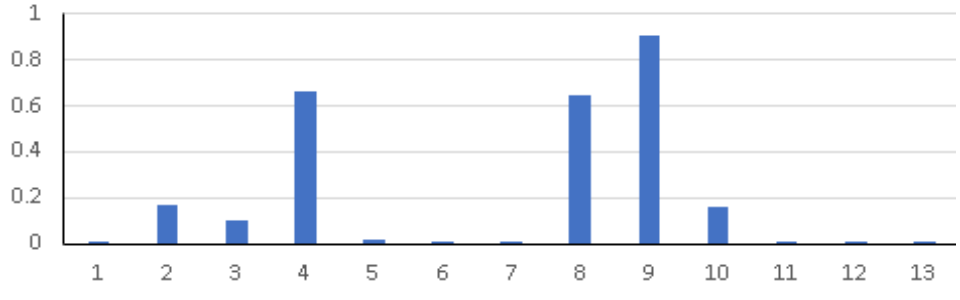

(b)

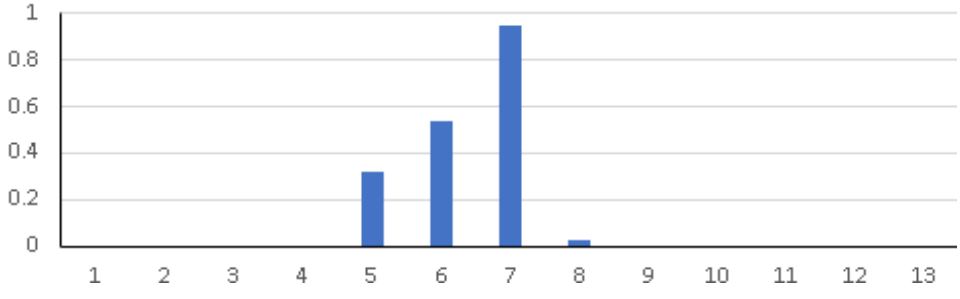

(c)

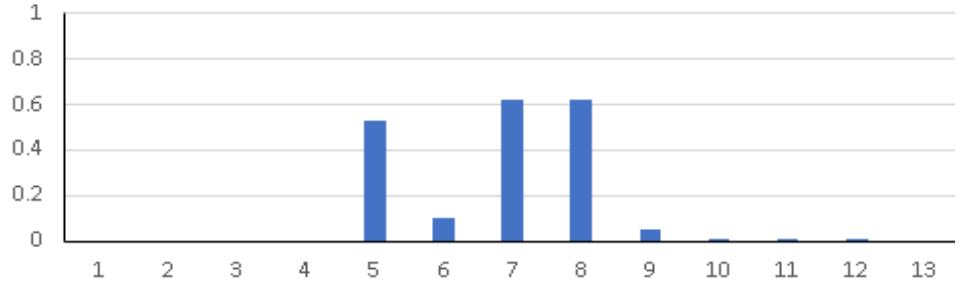

(d)

Note: The bar plots show the p-values vs. properties.

In addition to the comparison of data similarity, we also studied the resemblance of class disparity. Figures 3(c) and 3(d) depict the p-value distributions of real data and synthetic data. Again, the null hypothesis is that the two classes are drawn from the same distribution. Among the p-values of the real data, all but four properties are zero. The four non-zero properties show a fairly large correlation, which indicates possible redundancy for the purpose of differentiating the two classes. This distribution is also observed in Figure 3(d) for the synthetic dataset. Properties 5 through 8 have large p-values and the rest properties have zero or close to zero p-values, which exactly follow the distribution of the real data. The average p-values for the real dataset and the synthetic dataset are 0.141 and 0.148, respectively. This also confirms the resemblance of the synthetic dataset to the real dataset.

3.4 Computational efficiency

Although making predictions using a trained model is usually much efficient compared to developing a model via an iterative learning process, it is important to have a knowledge of how the proposed method responds to additional training examples when they become available. Figure 4 shows the time (in second) used by our proposed method and the base learners are SVM (using polynomial kernel) and neural network (20 hidden units and Levenberg-Marquardt backpropagation). The programs were implemented using Python 3 and executed in a computer with Intel i7-7500U CPU at 2.7 GHz, 16 GB memory, and Windows 10 64 bit.

Figure 4 Time used by GAN and the base learner SVM and neural network (see online version for colours)

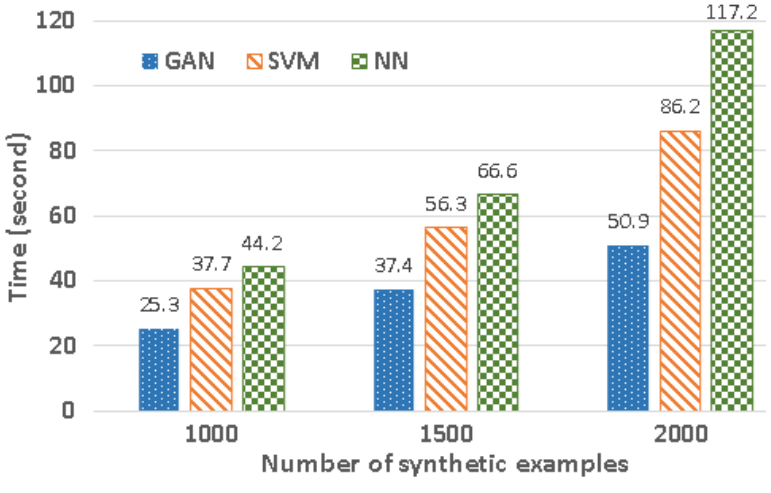

Note: The *x*-axis shows the number of additional synthetic examples generated by the GAN network.

The plot illustrates the average amount of time used to train a model by synthesising additional 1,000, 1,500 and 2,000 examples. We divided the time used to train the base learner (SVM or NN) and the GAN network to provide insights on how the extra examples increase the training workload. As the size increases, the amount of time used

by the GAN network increases linearly; whereas the amount of time used by training SVM (or NN) increases at an accelerated rate. The greater time increment of SVM (or NN) is partly caused by the supplemental training rounds using the synthetic examples and the example filtering process. A similar pattern is observed in the results by neural network. A much greater time increment was used in the training of NN. In the case of creating 2,000 synthetic examples, which increase the volume of training dataset by more than 30%, the total training time used by our proposed method is 137.1 seconds and 168.1 seconds when the base learner was SVM and NN, respectively. However, this is fairly efficient in real-world scenarios to create or update a model for response to extreme natural events. Hence, our method is applicable to scenarios that new real examples are acquired or synthetic examples are generated in near real-time.

4 Conclusions

Real data of power grids and many other strategic infrastructures are usually confidential and limited to research. To overcome the dearth of valuable examples in the event of disasters such as typhoons and floods, this paper presents a learning method that leverages GAN to generate synthetic examples to improve the characterisation of the strategic systems under extreme events. To obtain informative examples, the falsely classified examples by a base learner together with the examples that are correctly classified with low confidence are selected using a filtering strategy based on the significance of the training examples and are used in the training of a modulated GAN network. The synthetic examples are then generated using this GAN network to reinforce the learning of a model.

Experiments were conducted using the real data collected during the time when Typhoon Rammasun made landfall in Hainan. Our method demonstrated much-improved performance over predicting possible power grid faults. Compared to the baseline method, our method achieved an improvement by a rate of 8.9% in terms of the average sensitivity. In addition, the maximum improvement rate over the average balanced accuracy is 3.9%. It is, hence, evident that the positive change comes from the enriched training examples. When we look into the resemblance of the synthetic data to the real data, the average p-value for both minority and majority class is above 0.2, which is much greater than a typical significant level and provides strong support that the two datasets are probably following a similar, if not the same, distribution. The p-value distribution between classes in the real data and the synthetic data also exhibited strong agreement. The modulated GAN network produced credible synthetic data for supplementing the training of a reliable model. In the analysis of computational time, our method takes minutes to complete training of a base learner and the GAN network, which enables an efficient response to disasters such as typhoons with modern computing facilities including centralised or edge computing.

References

Arjovsky, M., Chintala, S. and Bottou, L. (2017) 'Wasserstein generative adversarial networks', in the *34th International Conference on Machine Learning*, Sydney, Australia, 6–11 August, Vol. 70, pp.214–223.

Chen, Y., Wang, Y., Kirschen, D. and Zhang, B. (2018) 'Model-free renewable scenario generation using generative adversarial networks', *IEEE Transactions on Power Systems*, Vol. 33, No. 3, pp.3265–3275.

Elhoseny, M., Tharwat, A., Yuan, X. and Hassanien, A.E. (2018) 'Optimizing k-coverage of mobile WSNs', *Expert Systems with Applications*, Vol. 92, pp.142–153, DOI: https://doi.org/10.1016/j.eswa.2017.09.008.

Elhoseny, M., Yuan, X., El-Minir, H.K. and Riad, A.M. (2014) 'Extending self-organizing network availability using genetic algorithm', in *Fifth International Conference on Computing, Communications and Networking Technologies (ICCCNT)*, Hefei, Anhui, 11–13 July, pp.1–6.

Fan, Y., Xia, Y., Liu, Y. and Yuan, X. (2016) 'Electricity cost management for cloud data centers under diverse delay constraints', in *IEEE 3rd International Conference on Cyber Security and Cloud Computing (CSCloud)*, Beijing, China, 25–27 June, pp.12–19.

Federal Energy Regulatory Commission, *Critical Energy/Electric Infrastructure Information (CEII) Regulations* [online] https://www.ferc.gov/legal/maj-ord-reg/land-docs/ceii-rule.asp (accessed 29 April 2020).

Goodfellow, I., Pouget-Abadie, J., Mirza, M., Xu, B., Warde-Farley, D., Ozair, S., Courville, A. and Bengio, Y. (2014) 'Generative adversarial nets', in *Advances Neural Information Processing Systems*, Montreal, Canada, 8–13 December, pp.2672–2680.

Gulrajani, I., Ahmed, F., Arjovsky, M., Dumoulin, V. and Courville, A. (2017) 'Improved training of Wasserstein GANs', in the *31st International Conference on Neural Information Processing Systems*, Long Beach, CA, 4–9 December, pp.5769–5779.

Mao, X., Li, Q., Xie, H., Lau, R.Y.K., Wang, Z. and Smolley, S.P. (2017) 'Least squares generative adversarial networks', in *IEEE International Conference on Computer Vision*, Venice, Italy, 22–29 October, pp.2813–2821.

Mathieu, M., Couprie, C. and LeCun, Y. (2016) 'Deep multiscale video prediction beyond mean square error', in *International Conference on Learning Representations*, San Juan, Puerto Rico, 2–4 May.

Reed, S., Akata, Z., Yan, X., Logeswaran, L., Schiele, B. and Lee, H. (2016) 'Generative adversarial text to image synthesis', in *International Conference on Machine Learning*, New York, NY, 19–24 June, Vol. 48, pp.1060–1069.

Yang, L., Chou, S. and Yang, Y. (2017) 'Midinet: a convolutional generative adversarial network for symbolic-domain music generation', in *International Society for Music Information Retrieval Conference*, Suzhou, China, 23–27 October.

Yi, Z., Zhang, H., Tan, P. and Gong, M. (2017) 'DualGAN: unsupervised dual learning for image-to-image translation', in *IEEE International Conference on Computer Vision*, Venice, Italy, 22–29 October, pp.2849–2857.

Yuan, X. and Abouelenien, M. (2015) 'A multi-class boosting method for learning from imbalanced data', *International Journal of Granular Computing, Rough Sets and Intelligent Systems*, Vol. 4, No. 1, pp.13–29.

Yuan, X., Xie, L. and Abouelenien, M. (2018) 'A regularized ensemble framework of deep learning for cancer detection from multi-class, imbalanced training data', *Pattern Recognition*, Vol. 77, pp.160–172, DOI: https://doi.org/10.1016/j.patcog.2017.12.017.